

## STUDY OF THE PICKLABILITY OF 1.8 mm HOT-ROLLED STEEL STRIP IN HYDROCHLORIC ACID

M.J.L. GINES<sup>a</sup>, G.J. BENITEZ<sup>a</sup>, T. PEREZ<sup>a</sup>,  
E. MERLI<sup>b</sup>, M.A. FIRPO<sup>b</sup> and W. EGLI<sup>b</sup>

<sup>a</sup> Centro de Investigación Industrial (CINI-FUDETTEC), CC 801, 2900 San Nicolás, Buenos Aires, Argentina  
yapgin@siderar.com

<sup>b</sup> Gerencia de Laminación (GELA-SIDERAR), CC 801, 2900 San Nicolás, Buenos Aires, Argentina

**Abstract** — After the hot rolling process the steel strip remains covered with an oxide layer (scale) which must be removed previous to the cold rolling process. The scale removal through the pickling process by hydrochloric acid (HCl) depends on both the scale structure and the conditions of the pickling bath (temperature, acid concentration, and dissolved iron concentration). This work is focused on picklability (decapability) studies accomplished in laboratory on hot-rolled steel strip, 1.8 mm thickness. The oxide amount was determined by weight difference of samples with and without acid pickling. The scale was characterized by X-ray Diffraction (XRD) and Scanning Electron Microscopy (SEM). The pickling or descaling time ( $t_d$ ) was determined using different bath conditions. Pickling kinetic studies were carried out being the pickled fraction ( $\alpha$ ) determined as a function of the immersion time. Expressions were obtained, allowing descaling time estimation under various pickling bath conditions. These expressions were used to estimate the maximum operation line speed that assures a complete descaling.

**Keywords** — Pickling, hydrochloric acid, oxide scale, hot-rolled strip, descaling.

### I. INTRODUCTION

During hot rolling process an oxide layer (scale) is formed on the surface of the steel. The aim of this process is to reduce steel slab thickness, typically from 230 mm, to strip products with thickness ranging from 1.2 to 12 mm. Usually, the steel strip temperature at the end of the hot rolling process (Finishing Temperature, FT) varies from 820 to 910°C, with an average of 870°C for strip having a thickness of 1.8 mm. Oxide scale formed at these temperatures is composed of three well defined layers (iron oxides), namely: a thick wüstite (approximate composition FeO) layer adjacent to the steel, then an intermediate magnetite (Fe<sub>3</sub>O<sub>4</sub>) layer, and finally a thin outermost hematite (Fe<sub>2</sub>O<sub>3</sub>) layer (Blazevic, 1987; Blazevic, 1996; Chen and Yuen, 2000a; Goode *et al.*, 1996; Hudson, 1991; Lecourt, 1996; Malik and White, 1981; Wei, 1990).

Following the finishing mill, the strip is quickly cooled by water spray on the run-out table and coiled at a temperature between 500-760°C. In this case, the coiling temperature (CT) is nearly 630°C. Finally, the steel

coil is cooled to room temperature by natural convection. While the strip is being cooled, the scale keeps growing, if there is oxygen supply. The same three layer structure is maintained until a temperature of 570°C is reached. However, when temperature drops below 570°C, wüstite becomes unstable and decomposes, leading to a mixture of iron and magnetite via a eutectoid reaction:



Depending on the temperature and the cooling rate, different oxide scale structure may build up within the original wüstite layer. At slow cooling rates, wüstite has enough time to decompose completely, forming a finely dispersed iron phase into magnetite, whereas at very rapid cooling rates the eutectoid transformation may be incomplete. Intermediate cooling rates lead to domains of undecomposed wüstite into the iron-magnetite matrix (Blazevic, 1987; Blazevic, 1996; Chen and Yuen, 2000a; Goode *et al.*, 1996; Hudson, 1991; Lecourt, 1996; Wei, 1990; Yamaguchi *et al.*, 1994). Besides, the cooling rates could be quite different depending on the locations in the coil (Chen and Yuen, 2000b).

In brief, the scale structure will be influenced by different processing parameters, such as the finishing and coiling temperatures, the cooling rate, and the conditions under which the coils are stored. Therefore, the scale structure will not be uniform throughout the coils, and variations are observed both across the width and along the length of the strip (Chen and Yuen, 2000a; Lecourt, 1996).

The scale must be removed previous to the cold rolling process, since it may produce operative problems and qualitative defects in the material. Effective scale removal is essential for the success, not only of cold rolling, but also of the subsequent annealing and coating operations (Lecourt, 1996). In order to get rid of these oxides, the steel strip is submitted to a critical process called pickling. The continuous pickling process consists in the immersion of steel strip in a series of tanks containing a hydrochloric (HCl) or sulphuric acid (H<sub>2</sub>SO<sub>4</sub>) hot aqueous solution. Hydrochloric acid is the most used acid. The choice between these two acids is complex and will not be considered in detail. However, it should be mentioned that hydrochloric acid shows a faster pickling rate than sulphuric acid, shortening the process time.

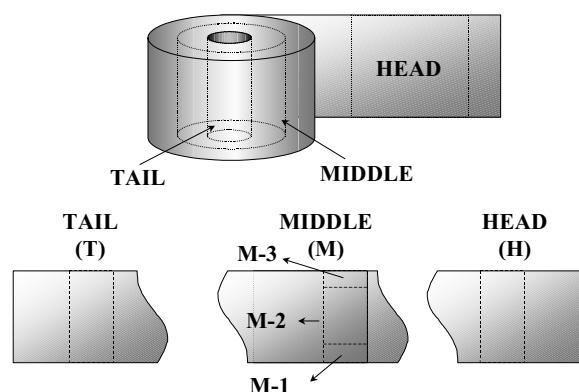
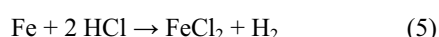
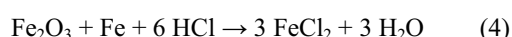
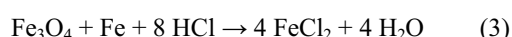


**Fig. 1:** Scheme of the locations of the samples in the hot-rolled steel strip.

The different iron oxides and metallic iron react with hydrochloric acid leading to ferrous chloride ( $\text{FeCl}_2$ ), water, and hydrogen. The chemical reactions are:



Reaction (5) is undesirable, and is avoided by adding an inhibitor. If no inhibitor is used to reduce the attack of the acid on the base metal, excessive weight loss may occur as well as a roughened surface and a reduction in the strip's average thickness (Hudson, 1991; Lecourt, 1996).

The pickling rate depends on two types of parameters: the product and the pickling bath characteristics (Lecourt, 1996). The former includes the characteristics of the steel, structure and thickness of the scale, which depends on the hot-rolled conditions (Chen and Yuen, 2000a; Chen and Yuen, 2000b; Lecourt, 1996; Wei, 1990; Yamaguchi *et al.*, 1994). The latter takes into account, particularly the chemical composition and temperature (Goode *et al.*, 1996; Hudson *et al.*, 1967; Hudson, 1982; Hudson, 1991; Kuhn, 1996; Lecourt, 1996; Lee *et al.*, 1997; Quantin, 1985; Yamaguchi *et al.*, 1994).

The knowledge of the relationship between pickling rate, scale structure, and the process variables is of industrial importance, since it allows to optimize the operation of the process line and to improve its productivity. In this work, and in an attempt to obtain more insight on the relationship among scale structure, pickling process variables and pickling time, several aspects were focused on: the characterization of the oxide layer on 1.8 mm hot rolled steel strip as a function of the location in the coil; the decapability at different positions of the coil (accomplished in laboratory); and the attain-

ment of expressions linking descaling time with process variables, allowing the estimation of the maximum line speed compatible with a complete descaling.

## II. METHODS

### A. Materials

The material used in this study was a commercial hot-rolled steel strip processed with finishing and coiling temperatures of 870 and 630°C, respectively. Steel chemical composition is given in Table 1.

Along the length of the strip, the samples were taken from the head (sample H), middle (sample M), and tail (sample T) of the coil. Also, the middle portion was split up in three parts across the width (M-1, M-2, M-3) as shown in Fig. 1. Each portion was cut in small samples, sized 3 x 3 cm<sup>2</sup> in order to carry out the physico-chemical characterization of the scale and the pickling experiments.

### B. Scale characterization

Scale composition was determined by X-ray diffraction (XRD). The scale morphology of the surface and of the cross-section of the samples was observed by scanning electron microscopy (SEM). The scale thickness was also measured by cross sectional observation.

XRD spectra were collected using an *X'PERT Philips* diffractometer and monochromatic  $\text{CuK}_\alpha$  radiation. Micrographs were obtained using an *XL 30 CP Philips* electronic scanning microscope. Semiquantitative chemical composition was determined by electron dispersive spectroscopy (EDS) with an electron probe (EDAX) attached to the microscope.

### C. Determination of the amount of oxide layer on hot-rolled steel strip

The amount of oxide on the hot rolled steel strip was determined by measuring the coupon weight before and after pickling. The coupons (3 x 3 cm<sup>2</sup>) were submitted to a thermostated and stirred batch reactor containing the pickling bath. The acid solution was taken from the pickling line tank, which contains pickling inhibitor. The pickling conditions were: 7.2 g HCl / 100 ml, 8.5 g Fe / 100 ml, 80-90°C. The scale amount ( $W_{\text{scale}}$ ) is expressed in kg . m<sup>-2</sup>.

### D. Determination of descaling time

Pickling tests were carried out in order to measure the pickling or descaling time ( $t_d$ ) as a function of the conditions of the pickling bath such as temperature (T), acid concentration ( $C_{\text{HCl}}$ ), and dissolved iron concentration ( $C_{\text{Fe}}$ ). Pickling time is defined as the time required for complete scale removal from the steel surface.

In a typical test, the hot rolled steel coupon was manually dipped in a well-stirred thermostated batch reactor containing the hot acid bath. Bath temperature was controlled to  $\pm 1^\circ\text{C}$  in the range 80-90°C, acid con-

**Table 1.** Chemical composition. Commercial hot-rolled steel strip, 1.8 mm thickness.

Element	C	Si	Mn	S	P	Al
%	0.083	0.017	0.41	0.010	0.011	0.37

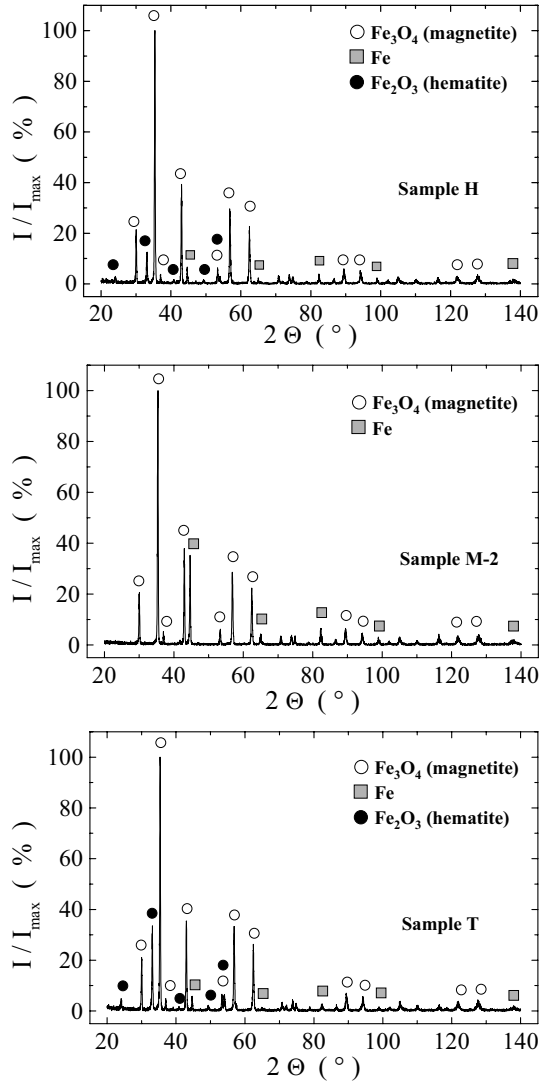


**Fig. 2:** X-ray diffraction patterns of the scale on 1.8 mm hot-rolled steel strip as a function of the location at the coil.

centration range was 3-11 g HCl / 100 ml, and the ferrous ion ( $\text{Fe}^{2+}$ ) concentration was varied from 4 to 12 g Fe / 100 ml. In order to achieve these concentrations, acid solutions were taken from the pickling line tanks, and were modified by adding fume HCl solution and/or  $\text{Fe}^{2+}$  (as  $\text{FeCl}_2 \cdot 4\text{H}_2\text{O}$ , reagent grade).

Before each test, the bath concentration was determined by titration techniques. A commercial inhibitor was used (0.2 % v/v), in order to avoid or diminish the action of the acid on the base steel.

The descaling time was determined by visual inspection using the trial and error method. The measures had an error of  $\pm 1$  s.

#### E. Pickled fraction ( $\alpha$ ) measurements

In order to determine the pickled fraction the coupons were dipped in the pickling bath during different times. When the pickling process ended, the coupon was rinsed thoroughly with warm running water, carefully

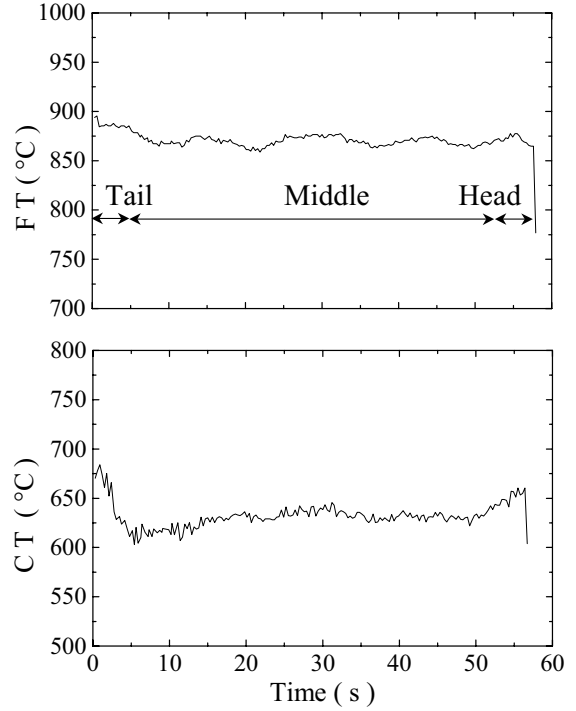


**Fig. 3:** Finishing temperature (FT) and coiling temperature (CT) along the coil.

dried, and immediately weighed. The loss of weight of the sample was used to estimate  $\alpha$ , which is defined as:

$$\alpha = (W_o - W_f) / W_{\text{scale}} \quad (6)$$

where  $W_o$  and  $W_f$  are the weights of the coupon before and after the pickling test, respectively. Thus, the evolution of the pickled fraction was determined as a function of dipping or residence time, using several HCl and Fe concentrations, and temperatures. All tests were carried out twice in order to ensure the consistency of the data.

### III. RESULTS AND DISCUSSION

#### A. Physicochemical characterization of the scale

XRD techniques were used for qualitative determination of the scale composition. XRD pattern for samples H (head), M-2 (middle-centre), and T (tail) are shown in Figure 2. M-1 and M-3 show the same pattern as M-2. All the samples contained magnetite ( $\text{Fe}_3\text{O}_4$ ) and iron (Fe) (Fig. 2). It must be emphasized that all the XRD spectra show no line attributable to retained wüstite ( $\text{FeO}$ ). This suggests that either the amount of  $\text{FeO}$  is very small or  $\text{FeO}$  was completely decomposed by the eutectoid reaction, as was shown in Eqn. (1) leading to Fe and  $\text{Fe}_3\text{O}_4$  formation (Blazevic, 1987; Blazevic, 1996; Chen and Yuen, 2000a; Goode *et al.*, 1996; Hudson, 1991; Lecourt, 1996; Wei, 1990; Yamaguchi *et al.*, 1994).

Across the middle of the coil (Samples M-1, M-2, M-3), no hematite was detected. This could be because hematite is present in trace amounts not detectable by XRD, or because of the limited (or even fully depleted) supply of oxygen inside the coil, after coiling, that

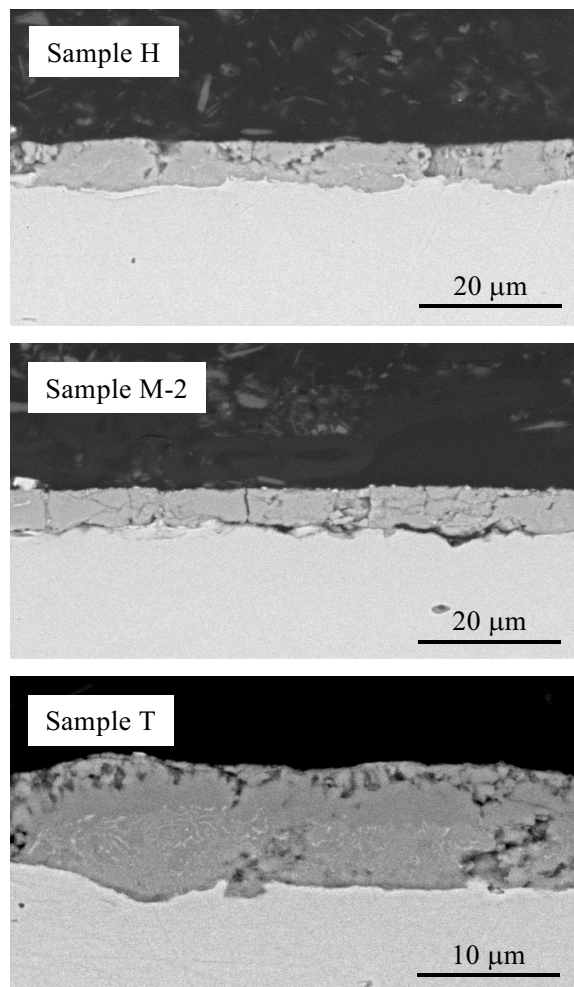


**Fig. 4:** Typical SEM micrographs of oxide scale in cross-section for different locations at the coil.

avoids further oxidation to hematite. This result is consistent with previous works (Chen and Yuen, 2000b). They showed that when cooling was carried out in nitrogen instead of air, the hematite layer remained extremely thin. A relatively thicker hematite layer is formed when the sample is cooled in air, especially when cooled from a very high temperature.

At the head (sample H) and tail (sample T) of coil hematite ( $\text{Fe}_2\text{O}_3$ ) was also detected. The amount of hematite is higher at the tail than at the head of the coil (Fig. 2). The presence of hematite at the tail could be due to the fact that finishing temperature (FT) and coiling temperature (CT) are greater than on other locations, as is shown in Fig. 3, and/or the oxygen pathways to the surface is attainable (Chen and Yuen, 2000b). Both facts would facilitate the oxidation process up to hematite. On the other hand, the hematite formation at head of the coil (tail of hot rolling process) might be due to the fact that this location of the coil is more exposed to air and water.

The scale morphology was examined on both cross-section and top views, using scanning electron microscopy. Figure 4 shows cross-section micrographs of the

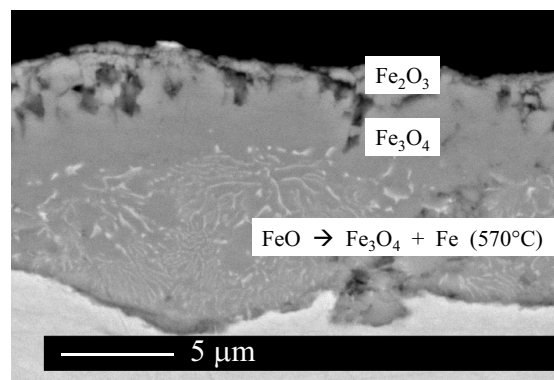


**Fig. 5:** Detailed SEM micrograph of sample T.

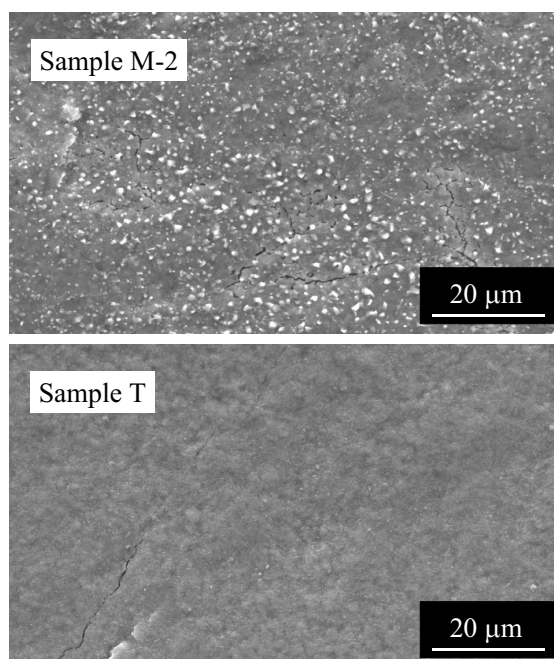


**Fig. 6:** SEM micrographs taken from the top view of the scale.

samples along the length of the strip. The micrographs show that the thickness of the oxide scale is relatively uniform, ranging from 6 to 10  $\mu\text{m}$ .

The lower thickness measured was at the head (6.4  $\mu\text{m}$ ), whereas the higher was at the coil (10  $\mu\text{m}$ ). Intermediate values were measured at the middle (6-8  $\mu\text{m}$ ).

These values agree with those published in the literature (Lecourt, 1996). The lower thickness at the head could be due to the fact that at the outer wraps of the coil, after hot rolling, the cooling rate is relatively high, avoiding further scale growth. Higher finishing temperature, at the head of hot-rolled strip (tail in pickling process), undergoes a high rate for scale formation. Several authors have studied the scale formation kinetic and they have found that the major factor in scale growth is temperature, followed by the time (Blazevic, 1987; Blazevic, 1996; Lanteri, 1996; Wei, 1990). The non-uniform thickness at the middle of the coil could be attributable to several reasons, namely: different cooling

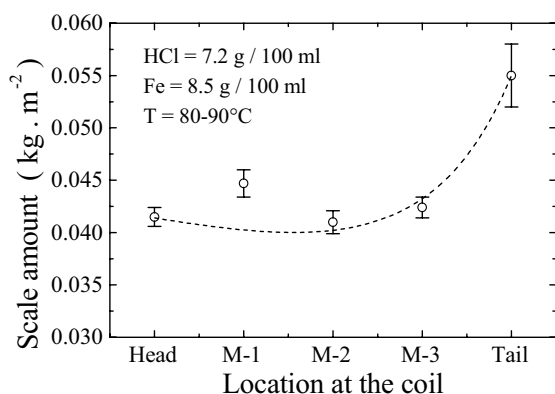


**Fig. 7:** Amount of the scale on 1.8 mm hot rolled steel strip as a function of the location at the coil.

rates and lack of oxygen supply because the position of the coil, and/or possibly non-homogeneous water cooling across the width of the coil at the run-out table. Despite the non-uniform thickness across the middle section, the scale structure was similar.

Figure 5 shows a detailed SEM micrograph in cross-section of the scale at the tail. The typical three layer composition is observed (Blazevic, 1987; Blazevic, 1996; Chen and Yuen, 2000a; Goode *et al.*, 1996; Hudson, 1991; Lecourt, 1996; Wei, 1990). The thin outermost layer is hematite (less than 1  $\mu\text{m}$  thickness), the intermediate layer is magnetite (2-3  $\mu\text{m}$  thickness), and the thick inner layer (6-7  $\mu\text{m}$ ) is composed of finely dispersed iron (bright white phase) and magnetite (grey phase). The latter layer was formed from wüstite, that undergoes a eutectoid reaction. The hematite and magnetite layers form because wüstite is oxidized to those higher iron oxides due to favorable conditions, such as high temperature and good supply of oxygen, and lower cooling rates. Once magnetite layer is formed, it continues to oxidize to form hematite (Lee *et al.*, 1997).

Figure 6 shows the SEM micrographs taken from the top view of the M-2 and T samples.

The morphology of these samples is quite different. Sample M-2 shows a huge amount of bright white nuclei (Fig. 6). These nuclei are also observed in samples H, M-1 and M-3, whereas only on sample T were absent (Fig. 6). EDS analysis reveals that the nuclei grown towards the surface are iron particles. This result is consistent with previous works, which showed the mechanism in which iron particles are formed during scale formation (Chen and Yuen, 2000a, b). Due to the fact that coiling temperature is high, and the oxygen supply

is not enough or is completely consumed inside the coil, further oxidation would take place during cooling at expense of the high oxides (hematite and magnetite). This would lead to further growth of the wüstite layer. When the high oxides are entirely depleted, the entire scale would be occupied by a single wüstite layer. As was described above, during cooling the wüstite layer decomposes leading to a mixture of magnetite and metallic iron. Iron particles observed on the scale surface were part of the wüstite decomposition products.

The amount of scale as a function of the position at the coil is shown in the Fig. 7. It is observed that the scale amount is quite uniform for all the locations at the coil, with the exception of the tail, where the amount is clearly greater (0.0550 kg · m<sup>-2</sup>). Also, on sample M-1 the amount is slightly greater (0.0447 kg · m<sup>-2</sup>) than on M-2 (0.0410 kg · m<sup>-2</sup>) and M-3 (0.0424 kg · m<sup>-2</sup>).

Scale thickness can be estimated from the scale amount and the magnetite density (5.18 g · cm<sup>-3</sup>), assuming that is the unique oxide that composes the oxide layer. The estimated and measured thicknesses show good agreement, and they are given in Table 2.

The higher scale amount at the tail (sample T) can be explained taking into account that the temperatures (FT and CT) are not uniform along the coil length (Fig. 3 and Table 2). It is observed that the FT as well as the CT are greater at the tail than in the rest of the coil. According to several authors (Chen and Yuen, 2000b; Lecourt, 1996), the FT has an important effect on the amount of oxide formed, while the CT has little influence. Instead, CT affects mainly the internal structure of the scale. Unpublished results obtained on 2.0 mm hot-rolled steel strip (FT ~ 870°C, CT ~ 720°C) also confirm these facts. We found that even though the CT is higher (by 90°C), the scale amount was slightly greater (0.0456 kg · m<sup>-2</sup>).

## B. Descaling time as a function of pickling bath conditions

Several pickling tests were done in a laboratory setup in order to measure the descaling time ( $t_d$ ), by employing different conditions of hydrochloric acid concentration ( $C_{\text{HCl}} = 3-11$  g / 100 ml), ferrous ion concentration ( $C_{\text{Fe}} = 4-12$  g / 100 ml), and temperature ( $T = 80-90^\circ\text{C}$ ). The hot-rolled steel coupons were taken from the middle of the coil (M-2 sample). A semi-empirical expression that relates the descaling time with  $C_{\text{HCl}}$  and  $T$  has been developed by Hudson (1982, 1991). The logarithm of descaling time is a linear function of the logarithm of hydrochloric acid concentration and the reciprocal of absolute temperature (in Fahrenheit degrees) of

**Table 2.** Scale thickness as function of the location at the coil.

Sample	FT (°C)	CT (°C)	Thickness <sup>(1)</sup> ( $\mu\text{m}$ )	Thickness <sup>(2)</sup> ( $\mu\text{m}$ )
H	872	650	6.4	8.0
M-1	870	630	8.6	8.6
M-2	870	630	7.4	7.9
M-3	870	630	6.2	8.2
T	890	660	10.0	10.6

<sup>(1)</sup> Measured from SEM micrograph. <sup>(2)</sup> Estimated from scale amount.

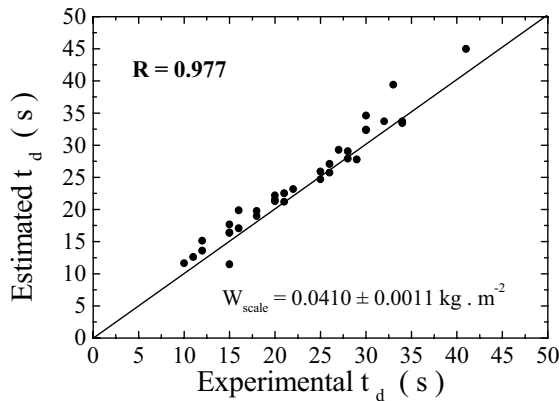


**Fig. 8:** Comparison between experimental and estimated descaling times.

the solution:

$$\log t_d = A + B \log C_{HCl} + \frac{D}{(T_F + 459)} \quad (7)$$

where A, B and D are the adjustable parameters. Usually, A and B are negative and D is positive.

Although, Hudson (1991) indicated that the influence of Fe content in solution (as FeCl<sub>2</sub>) is negligible unless it is higher than the limit of 34 g / 100 ml, other authors support that the detrimental effects of ferrous ions do not appear below 8 g / 100 ml (Lecourt, 1996). Therefore, the laboratory pickling results were fitted using an expression like Eqn. (7), but including a term that takes into account the ferrous ion concentration effect:

$$\log t_d = A + B \log C_{HCl} + \frac{D}{T} + S \log C_{Fe} \quad (8)$$

where t<sub>d</sub> is the pickling or descaling time, in s; A, B, D, and S are constant (parameters to be adjusted); C<sub>HCl</sub> is the HCl concentration, in g / 100 ml; C<sub>Fe</sub> is the concentration of Fe<sup>2+</sup>, in g / 100 ml; and T is the bath temperature, in K. The fitting results with 34 experimental data lead to the following parameters:

$$\begin{aligned} A &= -6.183 \pm 0.644 & D &= 2967 \pm 234 \\ B &= -0.776 \pm 0.038 & S &= -0.148 \pm 0.039 \end{aligned}$$

As shown in Fig. 8, the experimental descaling times were well fitted with those parameters.

Parameters in Eqn. (8) show that the descaling time has an exponential dependence with the temperature. The B parameter could be interpreted as the reaction order with respect to the HCl concentration. Due to the value of B is close to one, it can be said that the descaling time is inversely proportional to the HCl concentration. On the other hand, the concentration of Fe<sup>2+</sup> has a very slight positive influence on the descaling time.

**C. Descaling kinetics**

Kinetic studies were performed by weighing M-2 samples before and after the laboratory pickling tests. Experimental results were represented as curves of pickled fraction (α) as a function of time. The pickling tests were carried out varying the temperature and the HCl

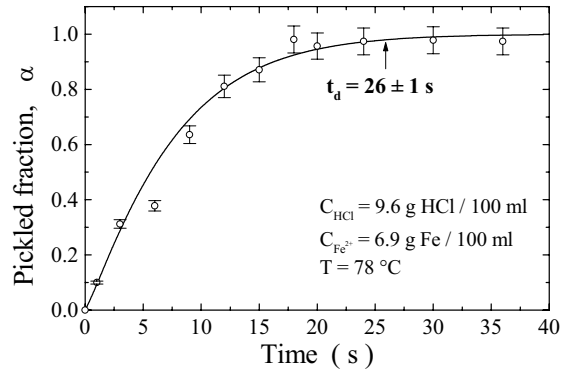


**Fig. 9:** Pickled fraction as a function of time.

concentration, one at the time. The ferrous ion concentration was not taken into account because its influence on t<sub>d</sub> is almost insignificant.

Figure 9 displays, as an example, the curve obtained for a particular bath condition. The curves show a S trend (sigmoidal plot). The same behavior was observed for all bath conditions. Similar curves were reported by several authors (Frenier and Growcock, 1984; Goode *et al.*, 1996; Yamaguchi *et al.*, 1994).

The experimental data were fitted employing the Johnson-Mehl-Avrami (JMA) type equation:

$$\alpha = 1 - \exp(-k_1 t^n) \quad (9)$$

where α is the pickled fraction, k<sub>1</sub> is the rate constant, t is the time, and n is the exponent of the time (Frenier and Growcock, 1984; Goode *et al.*, 1996; Yamaguchi *et al.*, 1994).

In order to simplify the analysis k<sub>1</sub> is split up into two factors, one of them depending on the solution temperature and the other on HCl concentration. As in this case the ferrous ion concentration has little effect on descaling time, it was not taken into account. The k<sub>1</sub> could be written as:

$$k_1 = f(C_{HCl}, T) = k(T) \cdot k'(C_{HCl}) \quad (10)$$

The temperature dependence of k is Arrhenius type which is typical of activated processes:

$$k(T) = C_1 \cdot \exp\left(-\frac{E_a}{RT}\right) \quad (11)$$

On the other hand, the functionality between k' and HCl concentration can be expressed using a power rate law equation:

$$k'(C_{HCl}) = C_2 \cdot C_{HCl}^m \quad (12)$$

where C<sub>1</sub> and C<sub>2</sub> are constants, E<sub>a</sub> is the apparent activation energy, R is the universal constant of gases, T is the absolute temperature, C<sub>HCl</sub> is the HCl concentration, and m is the reaction order. C<sub>1</sub> and C<sub>2</sub> constants can be grouped into one constant (A), named pre-exponential factor. Thus, Eqn. (10) becomes:

$$k_1 = A \cdot \exp\left(-\frac{E_a}{RT}\right) \cdot C_{HCl}^m \quad (13)$$

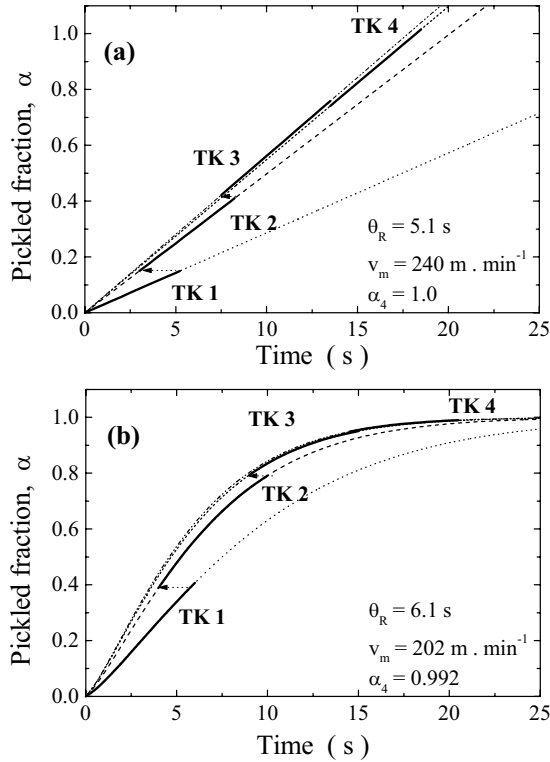


**Fig. 10:** Pickled fraction evolution along a four tank pickling line using: (a) linear relationship, Eqn. (14), and (b) sigmoidal JMA type equation, Eqns. (9) and (13).

Experimental data fitting was performed by multiple regression using Eqn. (9) and Eqn. (13), and leads to a unique function that links the pickled fraction with the bath conditions ( $C_{\text{HCl}}$  and  $T$ ). The obtained parameters were:

$$\begin{aligned} A &= 7563 & E_a &= 9.33 \text{ kcal} \cdot \text{mol}^{-1} \\ n &= 1.267 & m &= 0.86 \end{aligned}$$

The apparent activation energy ( $E_a=9.33 \text{ kcal mol}^{-1}$ ) obtained is similar to those reported in bibliography (Goode *et al.*, 1996). The reaction order  $m$  is close to those obtained in section III.B, and also agrees with the published values (Yamaguchi *et al.*, 1994).

#### D. Estimation of the maximum process speeds from laboratory pickling tests

From laboratory scale pickling test, maximum line speeds ( $v_m$ ) consistent with complete descaling under various tank conditions can be estimated. Assuming that the pickled fraction in a given tank  $j$  is directly proportional to the residence time ( $\theta_{Rj}$ ) of the steel strip in this tank, the value of  $v_m$  could be estimated with the follow-

ing equation (Hudson, 1991):

$$v_m = \sum_{j=1}^N (L_j / t_{dj}) \quad (14)$$

where  $L_j$  is the immersed strip length in tank  $j$ , and the  $t_{dj}$  can be estimated from Eqn. (8), knowing the conditions of each tank.

The value of  $v_m$  was also estimated in an iterative way by employing the pickled fraction expression (Eqns. (9) and (13)). To accomplish the calculation with this expression, it is necessary to take into account, that the JMA expression is asymptotic to 1. Due to this feature, the pickling time needed to achieve a unitary pickled fraction would be infinite. To solve this problem, it was considered that the strip was fully pickled for the  $\alpha$  values calculated from the sigmoidal expression introducing  $t_d$  values experimentally measured by visual inspection. The  $\alpha$  values vary from 0.973 to 0.992. Between these values, the most conservative is the upper limit, which implies less risk of underpickling.

Figure 10 shows an example of maximum line speed calculation, for the different tank conditions shown in Table 3. Hot-rolled steel strip used was 1.8 mm thickness.

Calculations, carried out using the linear approximation (Eqn. (14)), predict that using four tanks with the solution conditions showed in Table 3, would allow the process line to work at a maximum speed of  $240 \text{ m} \cdot \text{min}^{-1}$ . On the other hand, the maximum line speed estimated by using the sigmoidal curves (Fig. 10.b) was  $202 \text{ m} \cdot \text{min}^{-1}$ . These values agree with those used in pickling lines, for 1.8 mm hot-rolled steel strip.

## IV. CONCLUSIONS

The main conclusions of this study regarding the picklability of 1.8 mm hot-rolled steel strip in hydrochloric acid can be summarized as follows:

The amount and structure of the scale depends on the location at the coil, because of the variations in finishing and coiling temperatures, oxygen supply from air, and cooling rates.

The scale amount was nearly to  $0.043 \text{ kg} \cdot \text{m}^{-2}$  (thickness:  $8 \mu\text{m}$ ) along the length of the coil, but at the tail the scale amount was higher:  $0.055 \text{ kg} \cdot \text{m}^{-2}$  (thickness:  $10 \mu\text{m}$ ), because the finishing temperature was higher than on the other locations. Across the width, the amount varies slightly due to non-uniform cooling at the run-out table and/or different cooling rates.

Scale is mainly formed by magnetite and metallic iron, that were produced by a complete wüstite decomposition. At the head and tail of the coil, hematite was

**Table 3.** Bath conditions and descaling time in each tank.

Tank	$L_j$ (m)	$C_{\text{HCl}}$ (g / 100 ml)	$C_{\text{Fe}}$ (g / 100 ml)	$T$ ( $^{\circ}\text{C}$ )	$t_d$ (s)
1	20.5	3.7	6.1	89	28.6
2	20.5	6.0	4.5	90	19.5
3	20.5	8.0	5.1	87	17.9
4	20.5	9.0	4.4	95	18.6

formed because the high temperature and oxygen accessibility.

Descaling or pickling time depends on hydrochloric acid and ferrous ion concentrations, and solution temperature. Temperature is the most important variable, followed by hydrochloric acid concentration. The ferrous ion concentration has little relevance on descaling time.

A functional relationship of descaling time with hydrochloric acid and ferrous ion concentrations, and temperature was found. It was also found that the evolution of pickled fraction with residence time followed a sigmoidal curve kinetics. Both equations were used to estimate the maximum line speed for a complete pickling.

### REFERENCES

- Blazevic, D.T., "Rolled in scale - The consistent problem", *Proc. 4th International Steel Rolling Conf.*, Danville, France, **1**, 381-402 (1987).
- Blazevic, D.T., "Tertiary rolled in scale - The hot strip mill surface problem of the 1990's", *Proc. 37th MWSP Conf.*, ISS, **5**, 33-38 (1996).
- Chen, R.Y. and W.Y.D. Yuen, "A study of the scale structure of hot-rolled steel strip by simulated coiling and cooling", *Oxidation of Metals* **53** (5-6), 539-560 (2000a).
- Chen, R.Y. and W.Y.D. Yuen, "Effects of finishing and coiling temperatures on the scale structure and pickability of hot rolled strip", *Ironmaking and Steelmaking*, April, 47-53 (2000b).
- Frenier, W.W. and F.B. Growcock, "Mechanism of iron oxide dissolution - A review of recent literature", *Corrosion-NACE* **40** (12), 663-668 (1984).
- Goode, B.J., R.D. Jones and J.N.H. Howells, "Kinetics of pickling of low carbon steel", *Ironmaking and Steelmaking* **23** (2), 164-170 (1996).
- Goode, B.J., R.D. Jones, M. Evans and J.N.H. Howells, "Use of ultrasound in strip steel pickling process", *Ironmaking and Steelmaking* **24** (1), 72-78 (1997).
- Hayakawa, J., M. Ohtsuka, S. Nakagiri, T. Okano and T. Miki, "Operation of continuous pickling and tandem cold rolling mill (CP-4TM) at Sakai Works", *Memorial Symposium of the 100<sup>th</sup> Rolling Theory Committee Development and Prospect of Theory and Technology of Steel Rolling, ISIJ*, 251-258 (1996).
- Hudson, R.M., D.W. Brown and C.J. Warning, "Factors influencing the pickling time required for hot-rolled steel strip", *J. of Metals* **19** (3), 9-13 (1967).
- Hudson, R.M., "Pickling of iron and steel" in *Metals Handbook*, 9th edition, ASM, Vol 5, 68-82 (1982).
- Hudson, R.M., "Pickling of hot rolled strip: an overview", *Ironmaking and Steelmaking*, September, 31-39 (1991).
- Kuhn, A., "The process of steel pickling", *Steel Technology International*, 213-219 (1996).
- Lanteri, V., Surface reactions of steels during heat treatment in *The Book of Steel*, G. Béranger, G. Henry and G. Saiz (Eds.) Scierlog Editor, Intercept Ltd, Chapter 22, 536-556 (1996).
- Lecourt, S., Pickling in *The Book of Steel*, G. Béranger, G. Henry and G. Saiz (Eds.) Scierlog Editor, Intercept Ltd, Chapter 24, 584-595 (1996).
- Lee, K.H., R.J. Adams, R. Fassett, G. Jacque, M. Lewanski, T. Poquette, C.L. Nassarall and J. Pilling, "Hydrochloric acid pickling of coiled steel rods", *Proc. 1997 Steelmaking Conf.*, Chicago, IL, USA, **80**, 615-619 (1997).
- Malik, A.U. and D.P. White, "Oxidation of Fe-C alloys in the temperature range 600-850°C", *Oxidation of Metals* **16** (5-6), 339-353 (1981).
- Quantin, D., "Le mécanisme du décapage", *Mémoires et Etudes Scientifiques Revue de Métallurgie*, October, 537-558 (1985).
- Wei, F.-I., "The effect of scale structure on pickling of steel strip", *SEISI Quarterly* **19** (2), 20-24 (1990).
- Yamaguchi, S., T. Yoshida and T. Saito, "Improvement in descaling of hot strip by hydrochloric acid", *ISIJ International* **34** (8), 670-378 (1994).

Received: May 11, 2001.

Accepted for publication: June 7, 2002.

Recommended by Subject Editor A. L. Cukierman and Guest Editors E. L. Tavani and J. E. Pérez Ipiña.